

## Analysis of Atmospheric Plasma Spray Surface Composite Multilayer for Tire Mold Applications

Jan Novotný (0000-0001-7676-8495), Filip Mamoň (0000-0002-5658-9534), Štefan Michna (0000-0001-5893-5050), Tomáš Vlach (0000-0003-2326-4183)

Faculty of Mechanical Engineering, J. E. Purkyne University in Usti nad Labem. Pasteurova 3334/7, 400 01 Usti nad Labem. Czech Republic. E-mail: jan.novotny@ujep.cz

**This work investigates atmospheric plasma spraying (APS) coatings on aluminum molds used for truck tire vulcanization. Cobalt-based powders (MS1) and a NiAl interlayer combined with cobalt powders (MS1 + MS2) were deposited on AlMg3Mn alloy substrates. SEM/EDS analyses revealed that the NiAl interlayer improved adhesion, reduced chromium agglomeration, and enhanced elemental homogeneity. Vickers microhardness testing showed higher hardness values for MS1 + MS2 (457 HV 0.3) compared to MS1 (436 HV 0.3). Despite some residual cracks and porosity, their impact on performance was minimal. The study concludes that NiAl interlayer coatings significantly improve mold durability and operational life. Automated application and controlled-atmosphere spraying methods are recommended to further optimize coating properties for industrial use.**

**Keywords:** Atmospheric Plasma Spraying, Aluminum molds, Coatings, Microhardness, Vulcanization

### 1 Introduction

The Atmospheric Plasma Spraying (APS) process is based on the creation of an electric arc between a copper anode and a tungsten cathode within the torch, or between the torch and the coated component itself. The anode also serves to direct the resulting plasma stream of metallic composite particles. As a control and cooling medium, the systems use water or gas to reduce the temperature and remove excess energy.

The electric arc burns in an atmosphere of ionizing gas, typically argon. To increase the achievable arc power, it is supplemented with 20 to 50 volume percent helium or 5 to 15 volume percent hydrogen. The arc reaches extremely high temperatures, up to 15,000 K, and velocities of 1,000 m.s<sup>-1</sup>. The sprayed metallic composite powder is fed into the torch as the working medium. Upon contact with the plasma, the powder melts almost instantly and is accelerated outward from the torch toward the coated component. The powder particles impact the surface at speeds of up to 800 m.s<sup>-1</sup>, with a feed rate ranging from 50 to 150 g.min<sup>-1</sup> [1,2,3,4].

Due to the very high temperature of the arc, it is possible to use even highly refractory metals (or metal compounds) for spraying, such as tungsten carbides, titanium, tantalum etc. However, the temperature of the impacting particles is significantly lower than the temperature of the phase-structural transformations of the coated components, typically ranging between 80 and 120 °C [1,4].

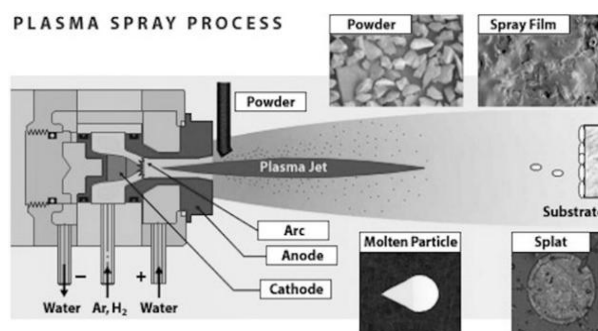


*Fig. 1 Schematic diagram of the atmospheric plasma spraying principle [5]*

### 2 Materials and methods

The powder of the sprayed material is melted by the plasma and accelerated toward the deposited surface. Due to the spraying parameters, a varying number of partially melted particles are formed and impact the surface. These particles, together with fully melted ones, create the coating surface. Insufficiently melted particles deteriorate the mechanical properties of the coating and reduce its adhesion to the base material of the component. The particles impacting the surface form lamellae, which build up the structure of the continuous coating layer. The thickness of the lamellae is influenced by the size and velocity of the impacting particles. Inside the coating, porosity and oxidation occur as a result of irregular particle impacts, uneven surface cooling, and contact with the surrounding atmosphere [2,6].

One of the main reasons for examining the microstructure of the resulting coating is to gain insight into the adhesion of the deposited layer to the substrate material or the formation of a diffusion bond with the substrate. The most desirable connection between the coating particles and the substrate is a diffusion bond, which depends on the melting temperature of the substrate, the plasma temperature, the velocity of the deposited particles, and other factors [7].

An important factor is also the adhesion mechanism, which involves the mechanical anchoring of particles to surface irregularities of the substrate. These irregularities are intentionally created during the preparation of the component for coating in order to improve adhesion. The deposited particles adhere to the irregularities, and upon cooling, they shrink and thus become anchored. The resulting bonding force can produce adhesion values of up to 70 MPa [8,9].

The part of the surface to which the deposited material adheres is called the "active zone." This zone is reduced by the presence of oxides, whether already present in the material or formed due to contact with the atmosphere. In cases where the substrate and coating material have the same or similar crystal structure, so-called epitaxy can occur — a process in which a crystalline layer grows between two existing crystal lattices.

The cause of this phenomenon may be van der Waals forces, diffusion occurring at higher process temperatures, as well as chemical reactions forming between the lamellae and the substrate material [2,10].

### 2.1 Plasma powder coating parameters

The experiment was designed based on the requirements of engineering practice within applied research. The base material of the samples is duralumin, and the sample surfaces were treated by corundum blasting. The surface roughness of the samples after blasting was [ $\mu\text{m}$ ]:  $R_a = 15.4$ ;  $R_z = 71.9$ .

The coated samples were divided into two groups. One group was coated exclusively with a powder mixture labeled MS1 (METALLIC MIXTURE 1), based on cobalt with additions of 28.5 % Mo, 17.5 % Cr, and 3.4 % Si.

The second group included an additional interlayer labeled MS2 (Ni 33.5 %, Al 66.5 %). To improve the adhesion of the coating to the substrate material, a NiAl interlayer was used. This layer is applied to the base material using the APS method, just like the subsequent MS1 layer. The coating layer was deposited onto the samples mounted on a rotating carousel (Fig. 2).

The powders were applied to the samples under the following conditions:

- Torch flame using argon and helium as process gases

- Voltage: 63 V
- Electric current: 560 A
- Powder feeder disc speed: 5 rpm
- Torch distance: 140 mm
- Spraying temperature: 1600 °C

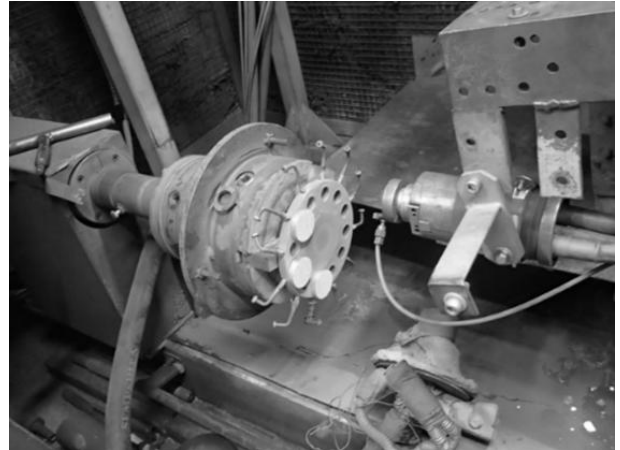


*Fig. 2 Sample placement in the rotating carousel*

## 3 Research and discussion

A scanning electron microscope (SEM), the TESCAN VEGA 3 XMU, equipped with a Bruker EDS analyzer, HKL Nordlys EBSD detector and a nanoindenter, was used. Within the microscopic analysis using electron microscopy, the individual structural constituents identified in the microstructure were analyzed by point, area, and line EDS analyses.

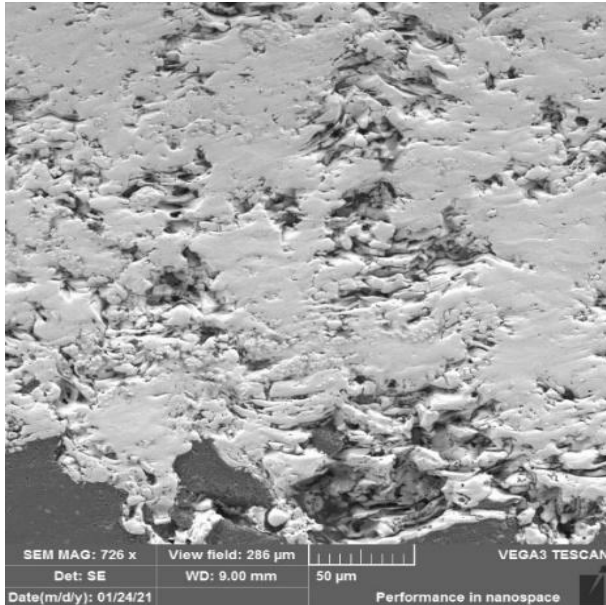
For the chemical analysis of different structural constituents, inclusions, and intermetallic phases, a TESCAN VEGA 3 scanning electron microscope fitted with a Bruker EDS analyzer was used. Point, area and line EDS analyses of the different structural constituents, inclusions, and intermetallic phases were performed using the scanning electron microscope.

### 3.1 Microstructure of deposited layers

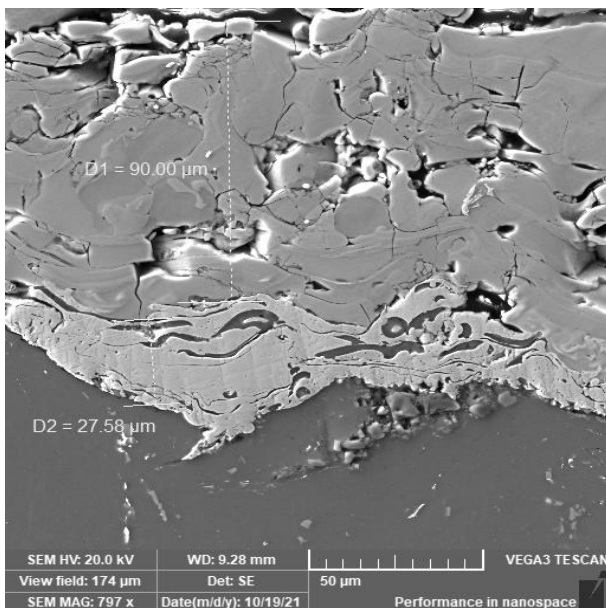
Figure 3 shows an SEM image revealing a high-quality bond between the deposited layer and the substrate surface, caused by the molten powder infiltrating surface irregularities and imperfections. In both cases, the increased porosity of the resulting coating is also clearly visible.

Figure 4 also shows a microstructure with a strong tendency to form lamellar layers. In the same image, a distinct transition can be seen between the substrate material, the NiAl interlayer, and the deposited TiMoAl coating. The purpose of the interlayer is to improve adhesion (preferably: bonding) between the substrate and the applied coating. Interlayers are used for their ability to adhere to the base surface even without significant surface roughening or other

surface treatments (such as degreasing, oxide removal, corrosion elimination etc.). The thickness of the applied interlayer typically ranges from 25 to 125  $\mu\text{m}$ . Materials commonly used for interlayers include primarily pure molybdenum, cobalt, and nickel-based alloys (such as NiAl). [9]



**Fig. 3** Microstructure of the deposited WC + Co layer (cross-section) on a substrate with good melt infiltration



**Fig. 4** Microstructure of the deposited NiAl + TiMoAl layer

### 3.2 Measuring the properties of applied powders

The main tool for evaluating the quality of deposited surfaces is the SEM (Scanning Electron Microscope) equipped with an EDS analyzer. Its use provides information not only about the structure of the deposited layer but also about its chemical composition — both overall and at the level of

individual structural components. EDS detectors can process this radiation to provide information about the chemical composition of the structure as a whole, as well as of its individual structural components (point, area, or line EDS analysis is possible). [11,12]

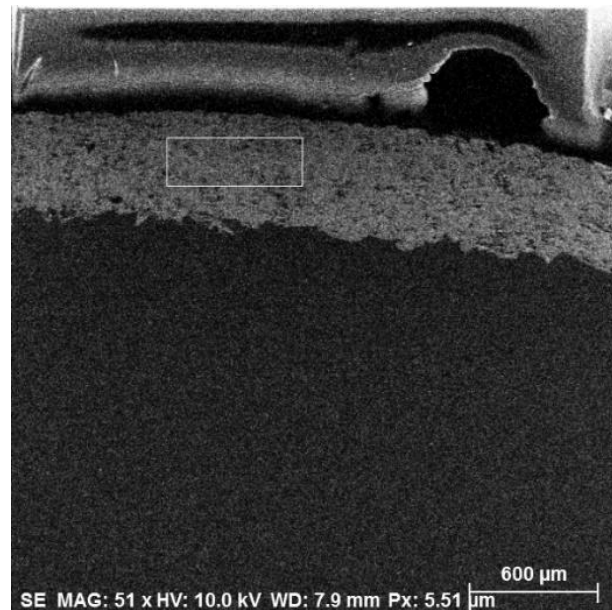


**Fig. 5** EDS analysis area of the WC + Co layer

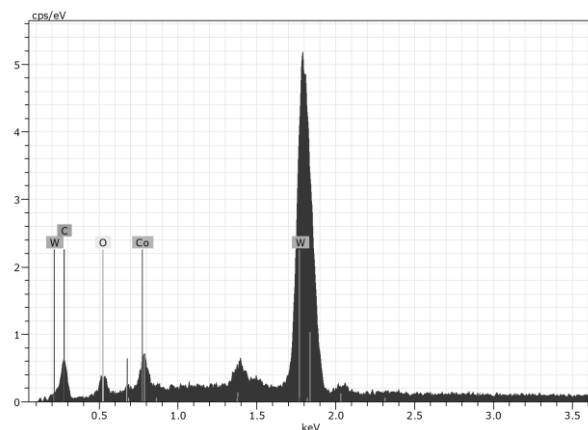


**Fig. 6** EDS analysis of elemental composition in the deposited WC + Co layer

### 3.3 Properties and requirements for deposited layers

The research activity investigates the process of applying cobalt-based powders onto aluminum molds and evaluates their suitability for coating molds used in the vulcanization of truck tire rubber. The APS method, along with the cobalt-based powder, was selected based on previous research conducted at the Faculty of Mechanical Engineering at UJEP and consultations with the industrial sector. The main goal is to assess the properties of these coatings with the aim of achieving longer mold service life, increasing the number of operating cycles between necessary cleanings, and simplifying maintenance.

For the purposes of this study, samples made of the same material as the aluminum molds (AlMg3Mn alloy) were coated to perform tests, the results of which serve as the basis for evaluating the practical applicability of the coatings.

The coating of the test samples and prototype molds was carried out by a specialized company equipped with atmospheric plasma spraying (APS) systems and focused on surface manufacturing and renovation using plasma and thermal spray techniques. Special test samples, modified for secure mounting in the coating equipment (Fig. 8), were prepared for testing. Prior to coating, the test samples were treated by grit blasting with corundum grains to increase surface roughness and thus ensure proper adhesion of the deposited powder. The actual coating of the test samples, shown in Figures 7 and 8, was performed mechanically using a plasma torch.

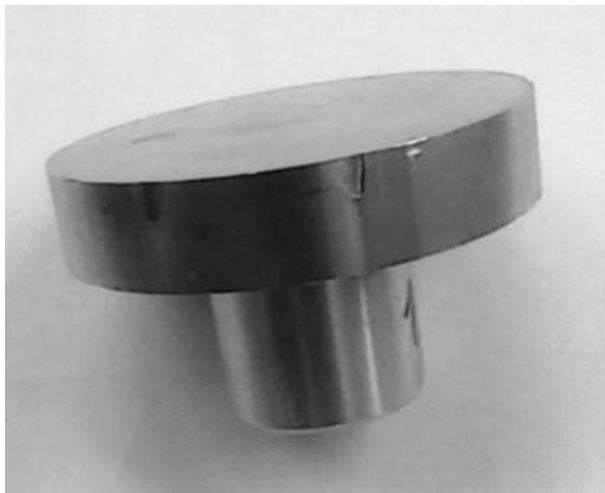


*Fig. 7* Base sample

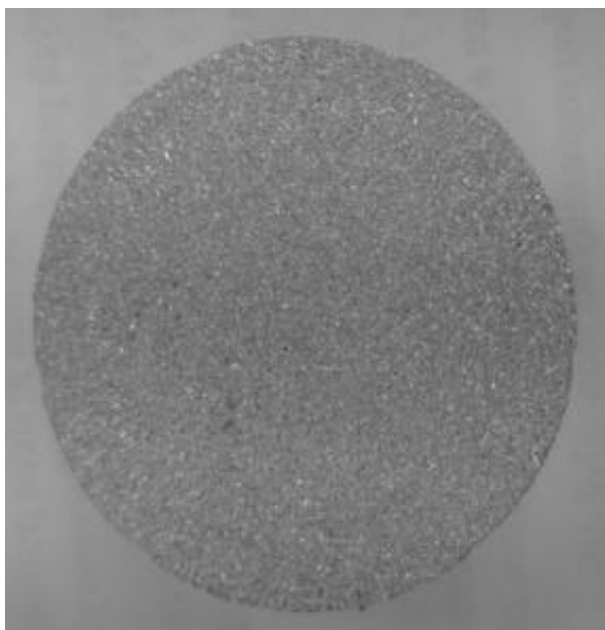


*Fig. 8* Base sample after corundum blasting

Powder mixture labeled MS1 (METALLIC MIXTURE 1) and its excellent coating properties are a result of the formation of hard precipitates (intermetallic Laves phases based on cobalt, molybdenum, and silicon), which are dispersed in a softer cobalt-based alloy matrix.

For the second group of the samples it was assumed that nickel acts as a thermal bridge between the aluminum and the cobalt-based powder, mitigating the differences in material properties, particularly melting temperature and thermal expansion. The aluminum content in the interlayer is significantly reduced due to evaporation during deposition; however, even the remaining aluminum substantially supports the bonding of the individual layers.

Figure 9 shows the distribution of the individual layers using an EDS analyzer. The base material, aluminum, is color-coded in yellow and is located at the bottom of the image. The MS2 (NiAl) interlayer is shown in yellow-orange, while the MS1 top coating is primarily highlighted in green at the top of the image. Analyses monitoring the composition of the powder after deposition on the base material were performed using the TESCAN VEGA 3 scanning electron microscope in combination with the EDS analyzer.

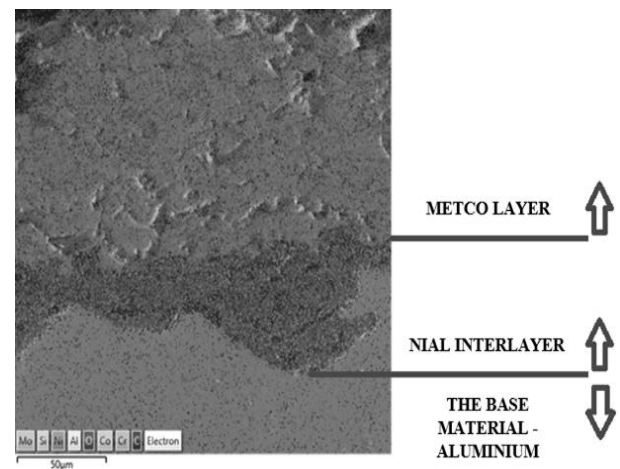


*Fig. 9* Distribution of individual layers: aluminum–NiAl–METCO

### 3.4 EDS analysis of coatings after plasma deposition

The EDS analysis of the MS1 coating focuses on selected regions of the analyzed layer, including the MS2 interlayer, and indicates a more uniform distribution of individual elements compared to the pure MS1 coating. There is no significant variation in cobalt or molybdenum concentrations with coating depth. Notably, the content of oxides increases toward the surface of the coating, along with carbon. The chromium content across individual spectra is evenly distributed. However, the interface between MS1 and MS2 shows the formation of cracks.

Figures 10–12 display images taken with an electron microscope. Figure 10 represents the average thickness of the applied layer, which is around 110  $\mu\text{m}$ .

In certain areas, however, the thickness reaches only 30 to 60  $\mu\text{m}$ , as shown in Figure 10. These variations in coating thickness are accompanied by visible depressions in the base material caused by the grit blasting of the substrate surface. Figure 10 also reveals a crack at the interface between the base material and the coating.

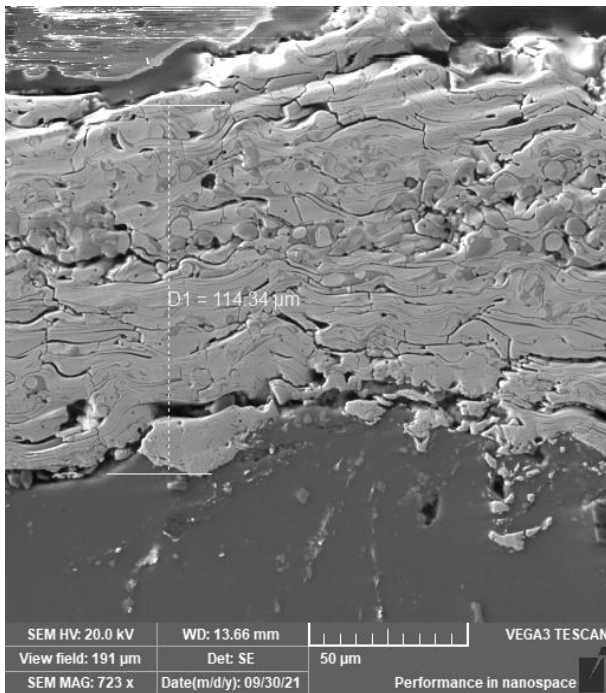


Fig. 10 SEM image of MS1

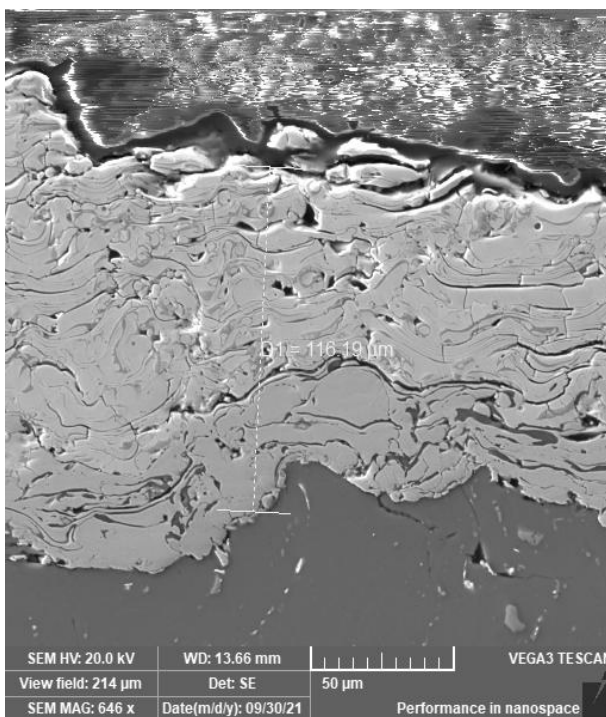


Fig. 11 SEM image of MS1

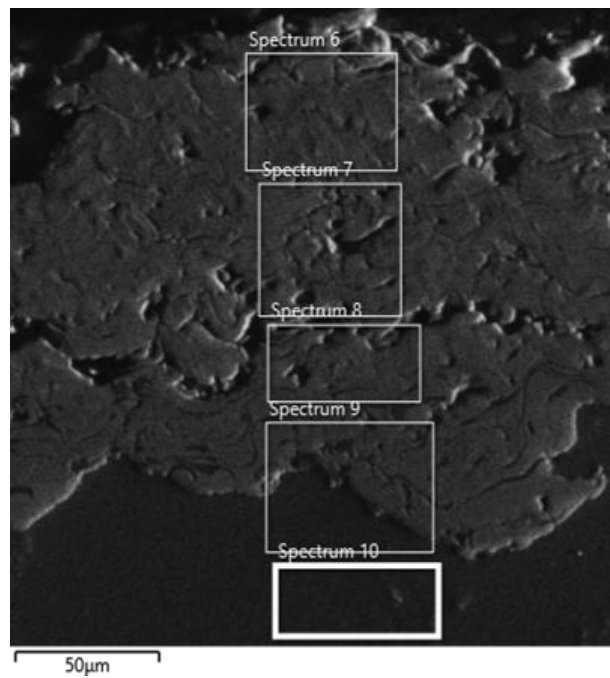


Fig. 12 Area EDS analysis of the MS1 + MS2 coating

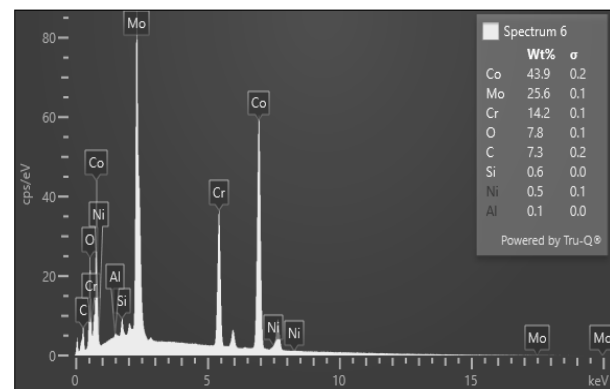


Fig. 13 EDS analysis of MS1 + MS2 in spectrum 6

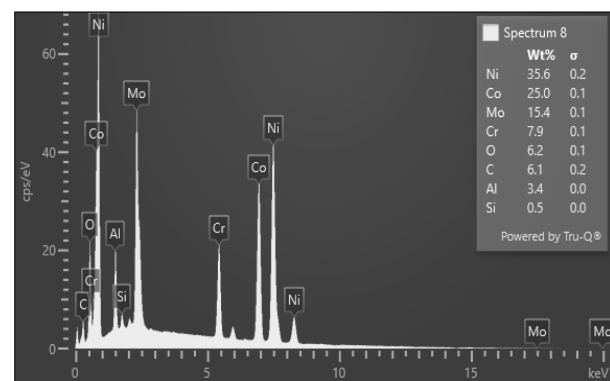
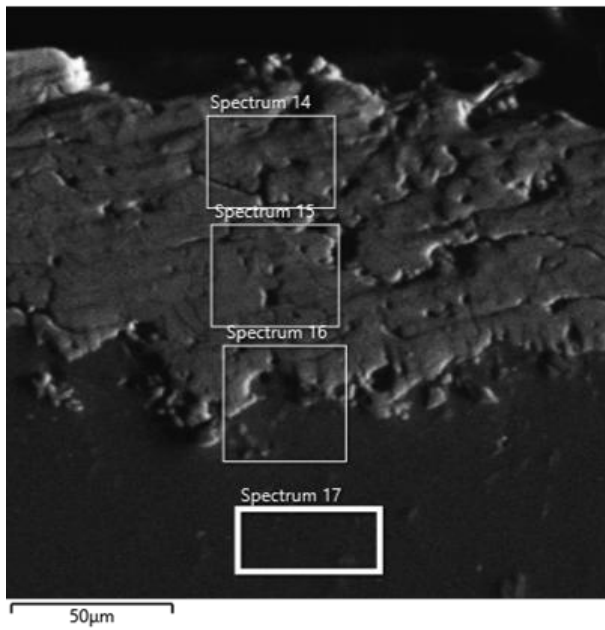
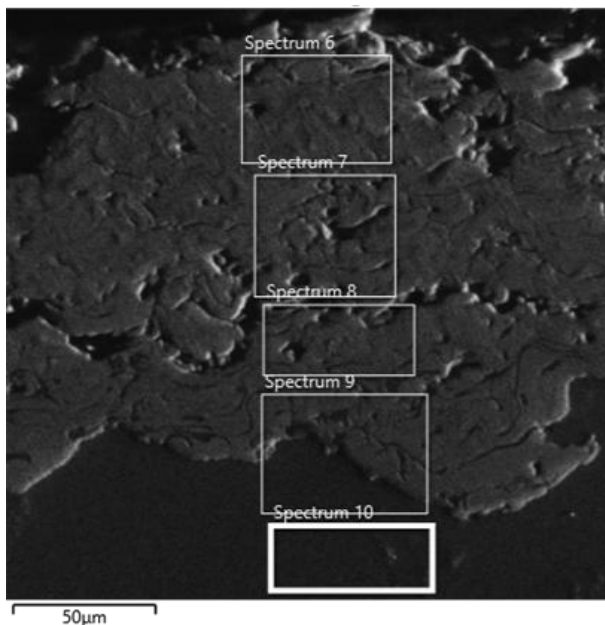


Fig. 14 EDS analysis of MS1 + MS2 in spectrum 8

Spectrum 8 on Figure 14 shows the transition area between MS1 and MS2. The structure and bonding of the individual layers can be observed in the SEM images, Figures 15 and 16. The structure shows improved adhesion to the base material with minimal porosity present.



**Fig. 15** SEM image of MS1 + MS2



**Fig. 16** SEM image of MS1 + MS2

### 3.5 Microhardness

The measurements were carried out using a microhardness test. This method is universally used for measuring the microhardness of a wide range of materials. It was chosen because its results are not dependent on the applied load magnitude. The method thus allows the testing to be adapted to thin surface layers without the results being influenced by the underlying substrate.

The principle is based on the penetration of an indenter — a diamond-shaped pyramid with a vertex angle of  $136^\circ$  — into the tested surface. The indenter is loaded perpendicularly to the surface at a constant and steady rate. After loading, it is unloaded, and the diagonals of the resulting indentation are measured.

Vickers hardness (HV) is then defined as follows [13–19]:

$$HV = 0.189 \frac{F}{d^2} \quad (1)$$

F...Force applied to the indenter [N],  
d...Arithmetic mean of the diagonals of the indentation [mm].

The test was performed using a Shimadzu HMV-2 microhardness tester, which was also used to capture images of the indentations. The measurements were carried out at room temperature. A load of 0.3 kg was selected for the test, as indicated by the notation “HV 0.3”. This load corresponds to approximately 3 N. This relatively low value was chosen to avoid exceeding the thickness of the coated layer, ensuring that the measured values reflect only the hardness of the coating itself.

The individual measurements were conducted on the samples in two perpendicular directions, with five measurements taken in each direction. Figure 17 illustrates the approximate distribution of the individual measurements on the sample.

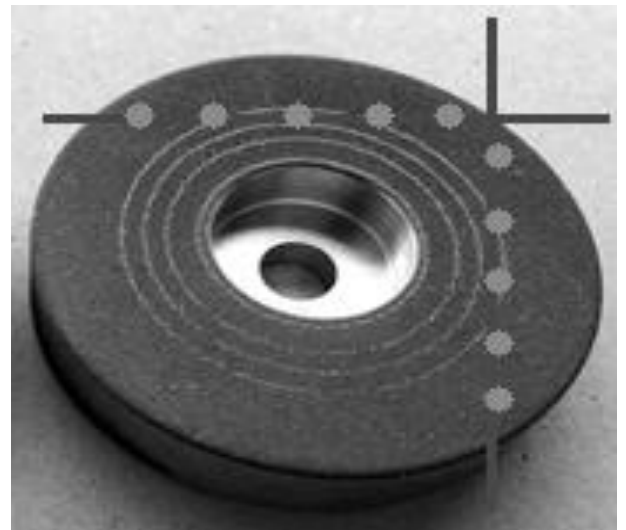


**Fig. 17** Visualization of individual measurement locations

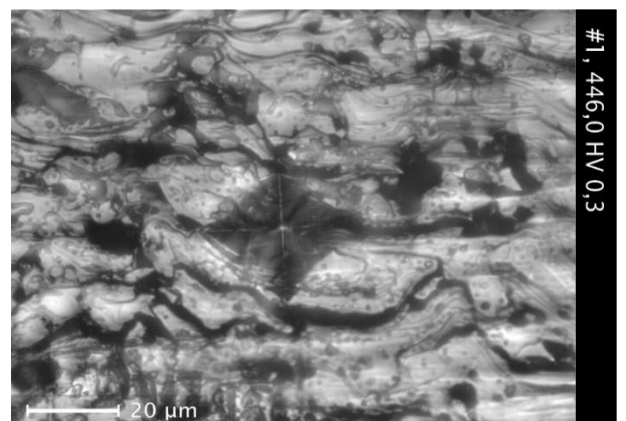


**Fig. 18** Indentation of the pyramid into the surface of the MS1 – MS2 coating

Figure 18 shows one of the indentations made to determine the microhardness values of the MS1 + MS2 coatings. A total of 10 tests were conducted for each of the coated components. The average measurement values for both coatings are presented in Table 1.

**Tab. 1** Average microhardness measurement values of the coatings

Measured coating	Average hardness value [HV 0.3]
MS1	435.94
MS1 + MS2	457.34

## 4 Conclusions

The goal of the experimental work was to evaluate the applicability of coating aluminum molds used for the vulcanization of tires. METCO 4800, a cobalt-based powder, was used for coating. Firstly, by itself, secondly, together with NiAl intermediate layer. Both layers were applied using the method of atmospheric plasma spraying. The desired result of these coats was to increase their lifespan, increased amount of work cycles between necessary cleaning of the mold and simplification of maintenance.

Following conclusions can be deduced based on the results:

Both cobalt and molybdenum evidently increased in concentration closer to main material. Application of the NiAl intermediate layer led to near complete reduction of these areas, pointing to the layers ability to enhance even element distribution across the structure and reach better heat flow during coating solidification.

EDS Mapping of METCO coating revealed the tendency of chrome to form clusters in which the concentration of chrome significantly increased. Application of NiAl interlayer led to near complete disappearance of these areas. The use of NiAl layer thus shows decrease in agglomeration of chrome to minimum.

Images made with SEM microscope shows emergence of cavitation and cracks in-between individually deposited materials, even after the use of NiAl intermediate layer. However, their occurrence was reduced with the use of the NiAl interlayer, and their persistence has no negative effect on the results of practical tests.

Mechanical properties of deposited coatings were investigated next.

The use of NiAl interlayer led to subtle increase of average measured micro hardness. This can be attributed to more even concentration of elements in coating due to the NiAl interlayer.

The NiAl intermediate layer used along METCO powder in coating resulted in more equally distributed elements in deposited layers, especially cobalt

and molybdenum and near complete reduction in chrome agglomeration. Furthermore, layer adherence was improved due to the creation of heat bridge in-between aluminum and METCO powder, resulting in form lifespan improvements and reduced wear and tear.

Based on performed test, following is recommended:

Automated application of coatings on forms, allowing superior coating application, more uniform thickness and therefore improvement in stress behavior. Adjustment of deposition parameters; torch distance, layer thickness, angle of deposition. Coating by hand creates problems controlling the process results. Automated application allows for change in coating parameters without the interference of human factor. Eventual controlled change in coating parameters allows for increase of the process quality.

Use of LPPS or VPS methods in coating deposition. Application in controlled atmosphere allows for reduction in oxides and carbon in coating and more even distribution of the powder. This way, higher coating densities can be achieved due to the absence of polluting elements and better coating properties can be achieved.

Despite the shortcoming, that the coating showed during the analyses, based on the results of the test performed, the use of the METCO + NiAl coating can be recommended for application on vulcanization molds in production.

## Acknowledgement

*This manuscript was created with the support of the project: NANOTECH ITI II., OP VVV Project with reg. No CZ.02.1.01/0.0/0.0/18\_069/0010045.*

## References

- [1] Plazmové depozice povlaků [online]. České vysoké učení technické, 2012. Available from: [http://fyzika.fs.cvut.cz/subjects/pm/lectures/pm\\_prednaska8.pdf](http://fyzika.fs.cvut.cz/subjects/pm/lectures/pm_prednaska8.pdf)
- [2] PAWLOWSKI, L.. The Science and Engineering of Thermal Spray Coatings. Vol. 2. West Sussex: John Wiley & Sons Ltd., 2008. ISBN 978-0-471-49049-4
- [3] Žárové stříkání [online]. SIAD, 2020. Available from: <https://www.siad.com/cs/odvetvi/svarovani-a-rezani/pouziti/svarovani-trenim>
- [4] KAŠPÁRKOVÁ, K.. Žárové nástřiky biokeramiky. Brno, 2018. VUT v Brně, Fakulta strojního inženýrství, Ústav strojřenská technologie. Available from:

- <https://dspace.vutbr.cz/bitstream/handle/11012/83388/final-thesis.pdf?sequence=-1>
- [5] Plasma spray-coating, Science learning HUB. Available from: <https://www.sciencelearn.org.nz/resources/245-plasma-spray-coating>
- [6] DAVIS, J. R.. Handbook of Thermal Spray Technology. USA: ASM International, 2004. ISBN 0-87170-795-0
- [7] RIABINKINA, P., BATRAEV, I., ULIANITSKY, V., RUKTUEV, A., EMURLAEV, K., CHERKASOVA, N., MALYUTINA, Y., GOLOVIN, E., BATAEV, I. (2023). Particle/substrate interaction and coating structure formation during detonation spraying of copper powder on steel. *The International Journal of Advanced Manufacturing Technology*, 129, 5625-5642. doi: 10.1007/s00170-023-12594-5
- [8] KAFLE, A., LU, S., SILWAL, R., ZHU, W. (2025). A Review on Material Dynamics in Cold Spray Additive Manufacturing: Bonding, Stress, and Structural Evolution in Metals. *MDPI Metals*, 15(2), 187. doi: 10.3390/met15020187
- [9] PRASHAR, G., VASUDEV, H. (2024). A comprehensive review on the analysis of adhesion strength of cold spray deposits. *Results in Surfaces and Interfaces*, 16, 100263. doi: 10.1016/j.rsurfi.2024.100263
- [10] Epitaxe [online]. c2021 [citováno 19. 01. 2023]. Available from: <https://cs.wikipedia.org/w/index.php?title=Epitaxe&oldid=20305880>
- [11] SWAPP, S.. Scanning Electron Microscopy (SEM). In: *Science Education Resource center (SERC) at Carleton College* [online]. Carleton College, 2017. Available from: [https://serc.carleton.edu/research\\_education/geochemsheets/techniques/SEM.html](https://serc.carleton.edu/research_education/geochemsheets/techniques/SEM.html)
- [12] Skenovací elektronový mikroskop (SEM) [online]. Matca. Available from: <https://matca.cz/technologie/analyticke-metody/sem/>
- [13] ŠILDBERGER, R.. Optimalizace parametrů nástřiku elektrickým obloukem. VUT v Brně, fakulta strojního inženýrství, ústav strojírenské technologie. Available from: [https://www.vut.cz/www\\_base/zav\\_prace\\_soubor\\_verejne.php?file\\_id=7516](https://www.vut.cz/www_base/zav_prace_soubor_verejne.php?file_id=7516)
- [14] Metoda Vickers [online]. JD Dvořák s.r.o. Available from: <https://www.testsysteme.cz/metoda-vickers>
- [15] Využití metody Vickers v praxi [online]. JD Dvořák s.r.o. Available from: <https://www.testsysteme.cz/vyuziti-metody-vickers-v-praxi>
- [16] Měření tvrdosti v kostce metoda Vickers (kovové materiály) [online]. Metalco Testing s.r.o. Available from: <https://www.metalco.cz/mereni-tvrdosti-v-kostce-metoda-vickers/>
- [17] HREN, I., MICHNA, Š., NOVOTNÝ, J., MICHNOVÁ, L. (2021). Comprehensive analysis of the coated component from a FORD engine. *Manufacturing Technology Journal*, 21(4), 464-470. doi: 10.21062/mft.2021.058
- [18] MICHNA, Š., KNAISLOVÁ, A., SVOBODOVÁ, J., NOVOTNÝ, J., MICHNOVÁ, L. (2024). Possibility of Eliminating Iron in Aluminium Alloy through Sedimentation. *Manufacturing Technology Journal*, 24(5), 802-810. doi: 10.21062/mft.2024.082
- [19] NÁPRSTKOVÁ N, ŠRAMHAUSER K, HREN I, NOVOTNÝ J, SVIANTEK J.: Microscopic Wear Analysis of Indexable Inserts after Machining of 34CrNiMo6 Steel. *Manufacturing Technology*. 2023; 23(5):676-684. doi: 10.21062/mft.2023.077